



Figures and figure supplements

Islet vascularization is regulated by primary endothelial cilia via VEGF-A-dependent signaling

Yan Xiong *et al*

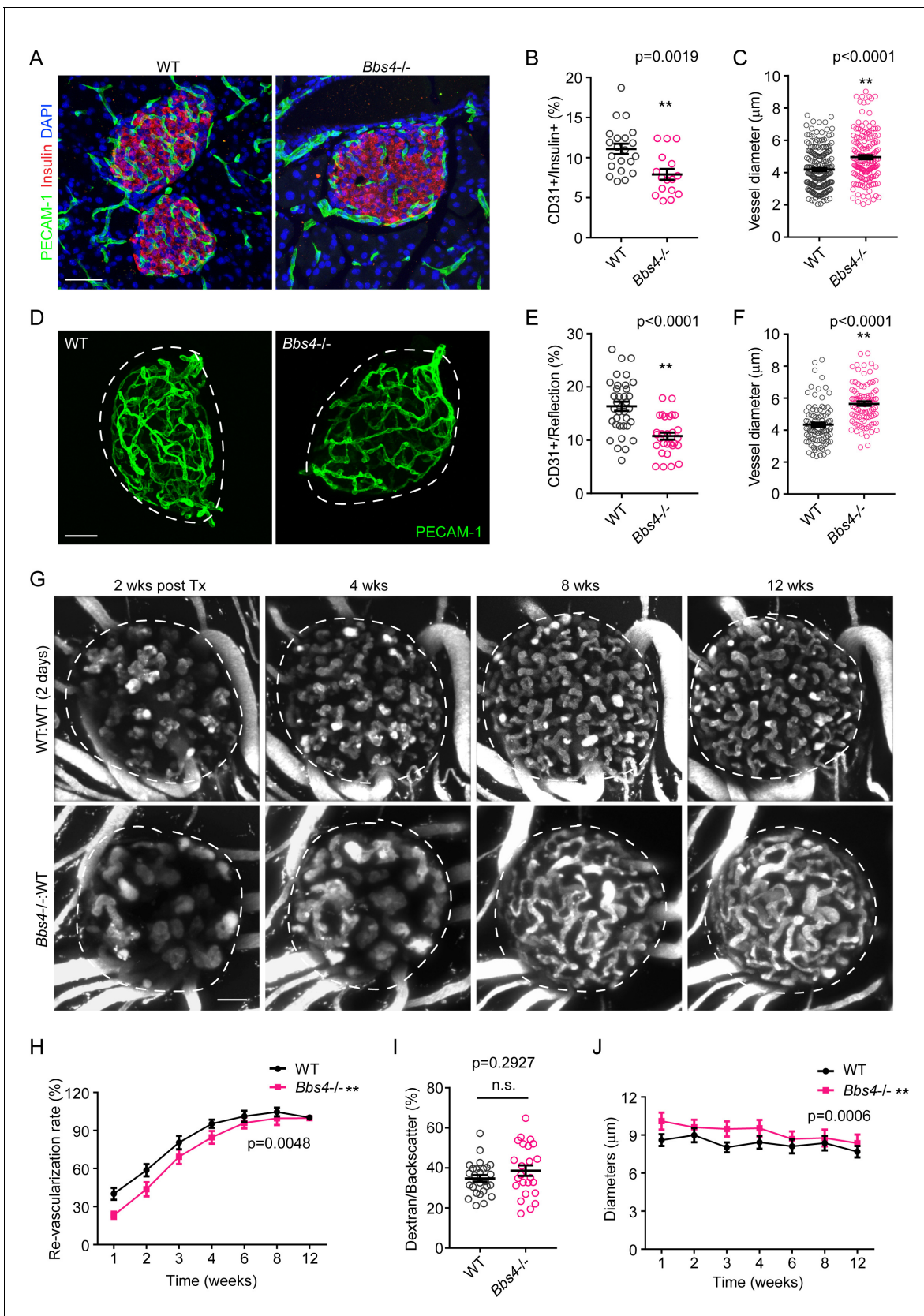


Figure 1. *Bbs4*^{-/-} islets show delayed vascularization and enlarged capillary diameter in the pancreas and the anterior chamber of the eye upon transplantation. (A) Immuno-fluorescence staining of pancreatic sections from 2-month-old wt and *Bbs4*^{-/-} mice showing islets (insulin, red) and intra-
 Figure 1 continued on next page

Figure 1 continued

islet capillaries (PECAM-1, green). (B–C) Quantification of relative intra-islet PECAM-1 positive volume, normalized to insulin-positive volume (B) and average intra-islet capillary diameters (C) in wt and *Bbs4*^{-/-} pancreatic sections. Individual data points are shown, ***p*<0.01, *n* = 8 for animals and *n* = 2–3 islets per animal. (D) Immuno-fluorescence staining of freshly isolated and fixed pancreatic islets from 2-month-old wt and *Bbs4*^{-/-} mice, showing PECAM-1 (green) labeled islet capillaries. (E–F) Quantification of relative PECAM-1 positive volume within each islet, normalized to islet volume estimated by backscatter signal (E) and average capillary diameters (F) in wt and *Bbs4*^{-/-} islets. Individual data points are shown, ***p*<0.01 by Mann-Whitney test, *n* = 3 for animals and *n* = 8–12 islets per animal. (G) Re-vascularization of 2 day-cultivated wt (upper) and *Bbs4*^{-/-} (lower) islets in wt recipient eyes at 2-, 4-, 8- and 12-weeks post-transplantation, visualized by intravenous injection of Texas Red-conjugated dextran. (H) Quantification of re-vascularization rates of wt and *Bbs4*^{-/-} islet grafts in wt recipients. Results are shown as mean ± SEM. (I) Relative vascular density of wt and *Bbs4*^{-/-} islet grafts at the end of 12 weeks post-transplantation. Individual data points are shown, n.s. means not significant by Mann-Whitney test. (J) Average diameters of newly formed capillaries in wt and *Bbs4*^{-/-} islet grafts in wt recipients. Results are shown as mean ± SEM, **p*<0.05, ***p*<0.01 by two-way-ANOVA, *n* = 6 for animals and *n* = 4–8 islets per animal. Islets were encircled by dashed lines. The same is for all the other figures. Scale bars: 50 μm.

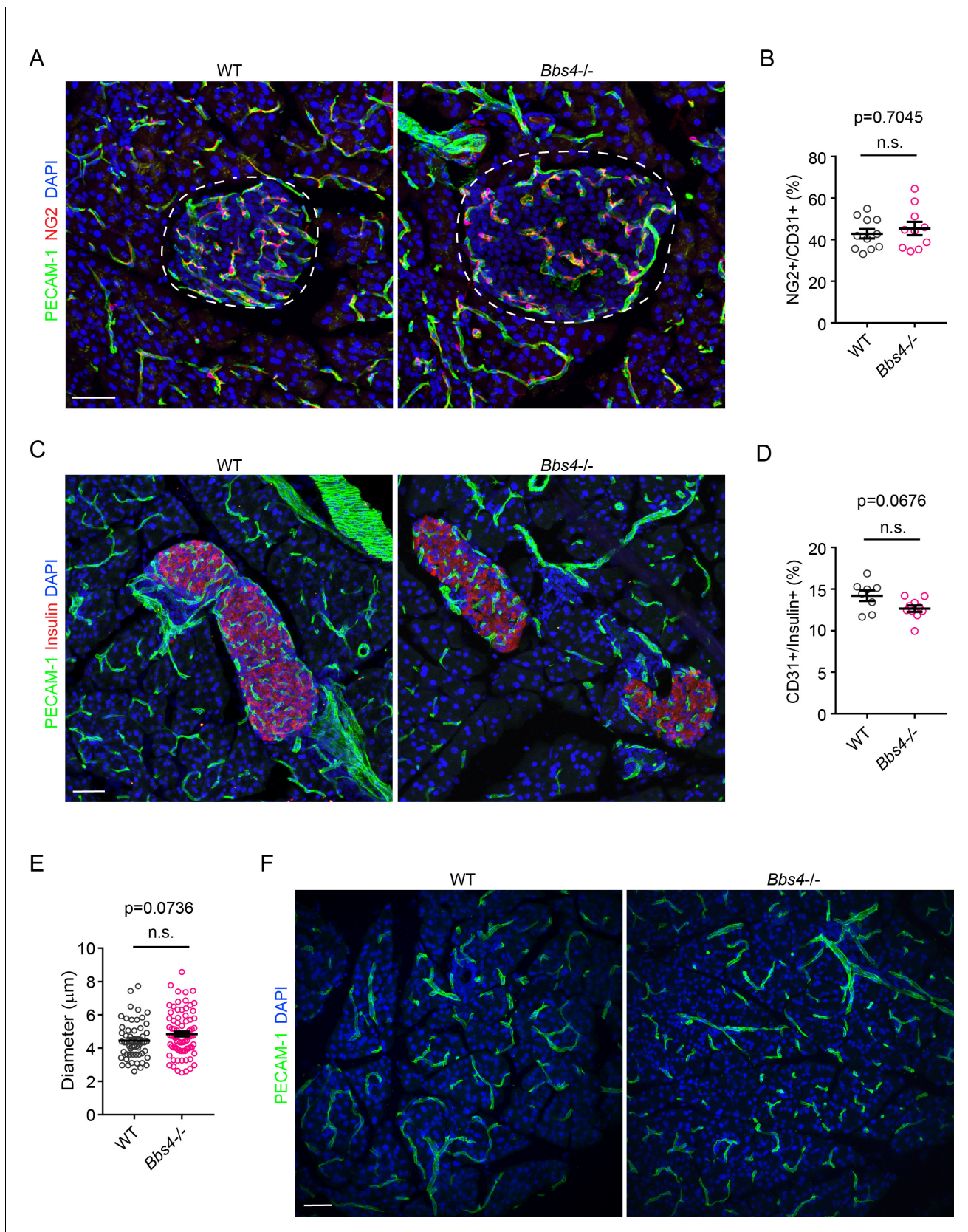


Figure 1—figure supplement 1. Pericyte coverage of intra-islet capillaries and capillary density in exocrine pancreas are not affected in *Bbs4*^{-/-} mice. (A) Immuno-fluorescence staining of pancreatic sections from 2-month-old wt and *Bbs4*^{-/-} animals showing pericyte coverage (NG2, red) on intra-islet capillaries (PECAM-1, green). Scale bars, 10 μm . (B) Quantification of pericyte coverage on intra-islet capillaries. (C) Immunofluorescence staining of pancreatic sections from 2-month-old wt and *Bbs4*^{-/-} animals showing pericyte coverage (PECAM-1, green) on intra-islet capillaries (Insulin, red). Scale bars, 10 μm . (D) Quantification of pericyte coverage on intra-islet capillaries. (E) Quantification of intra-islet capillary diameter. (F) Immunofluorescence staining of pancreatic sections from 2-month-old wt and *Bbs4*^{-/-} animals showing pericyte coverage (PECAM-1, green) on intra-islet capillaries (DAPI, blue). Scale bars, 10 μm . *n.s.*, not significant. *p*-values are indicated above the plots.

Figure 1—figure supplement 1 continued on next page

Figure 1—figure supplement 1 continued

capillaries (PECAM-1, green). (B) Quantification of surface ratio of NG2 positive area to PECAM-1 positive area. $n = 4$ for animals and $n = 2-4$ islets per animal. (C) Immuno-fluorescence staining of pancreatic sections from 4-month-old wt and *Bbs4*^{-/-} animals showing islets (insulin, red) and intra-islet capillaries (PECAM-1, green). (D–E) Quantification of relative intra-islet PECAM-1 positive volume, normalized to insulin-positive volume (D) and average intra-islet capillary diameters (E) in wt and *Bbs4*^{-/-} islets from 4-month-old animals. $n = 4$ for animals and $n = 2-4$ islets per animal. (F) Immuno-fluorescence staining of pancreatic sections from 2-month-old wt and *Bbs4*^{-/-} animals, showing PECAM-1 (green) labeled capillaries in exocrine pancreas. Individual data points are shown, n.s. means not significant by Mann-Whitney test. Scale bars: 50 μm .

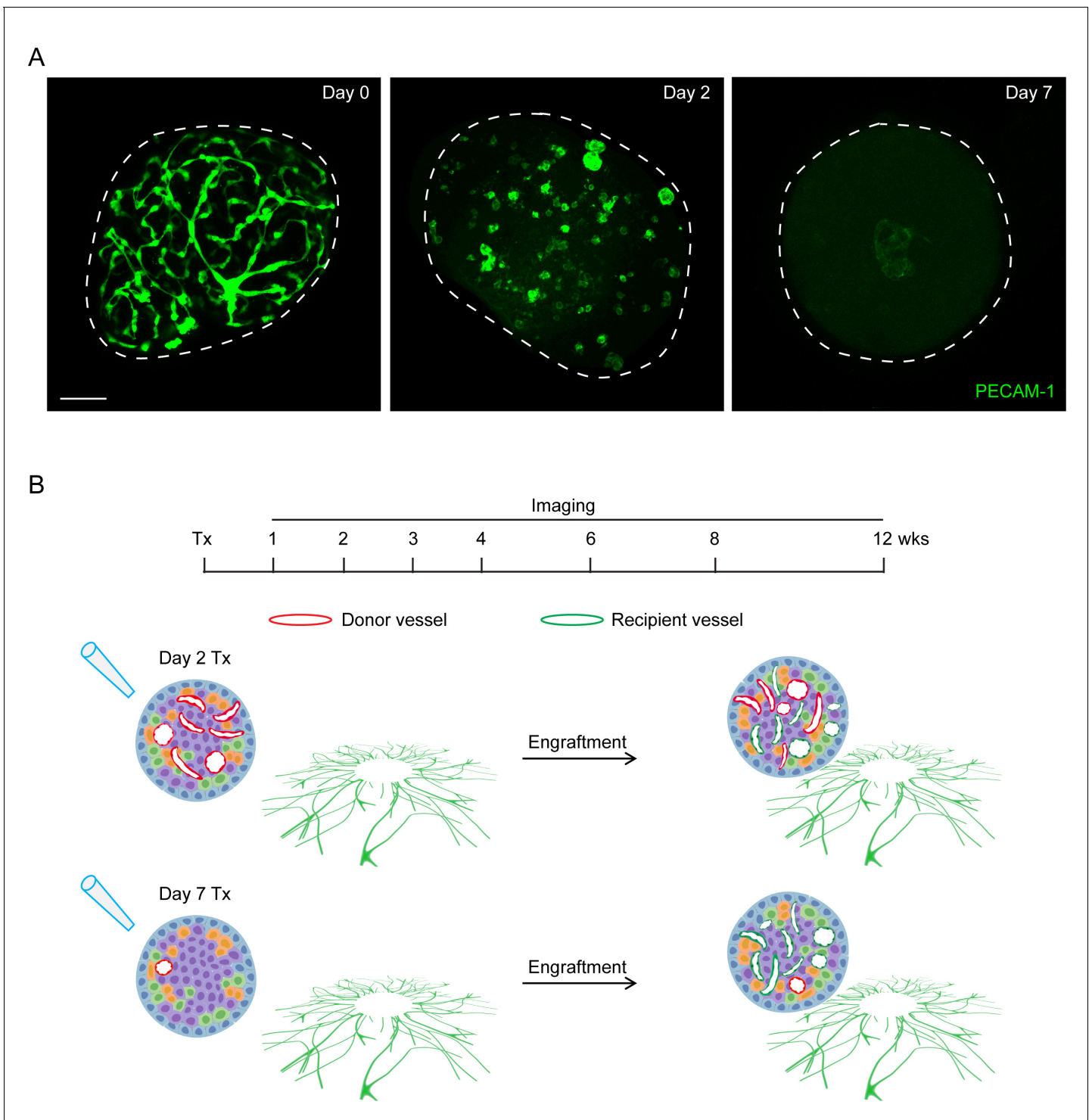


Figure 1—figure supplement 2. Number of donor endothelial cells participating in islet re-vascularization decreases under prolonged cultivation. (A) Remaining endothelial cells in islets which were freshly isolated (left), or cultured for 2 days (middle) or 7 days (right), indicated by whole islet PECAM-1 staining. Scale bar: 50 μ m. (B) Schematic illustration of two scenarios of islet revascularization in the anterior chamber of mouse eyes. Upper panel indicates that when transplanted after minimum in vitro culture, the newly formed islet microvasculature is composed of both donor islet vascular cells (red) and recipient cells (green). Lower panel indicates that when transplanted after prolonged culture, the number of donor islet vascular cell decreases, and islet re-vascularization is mainly derived from recipient cells.

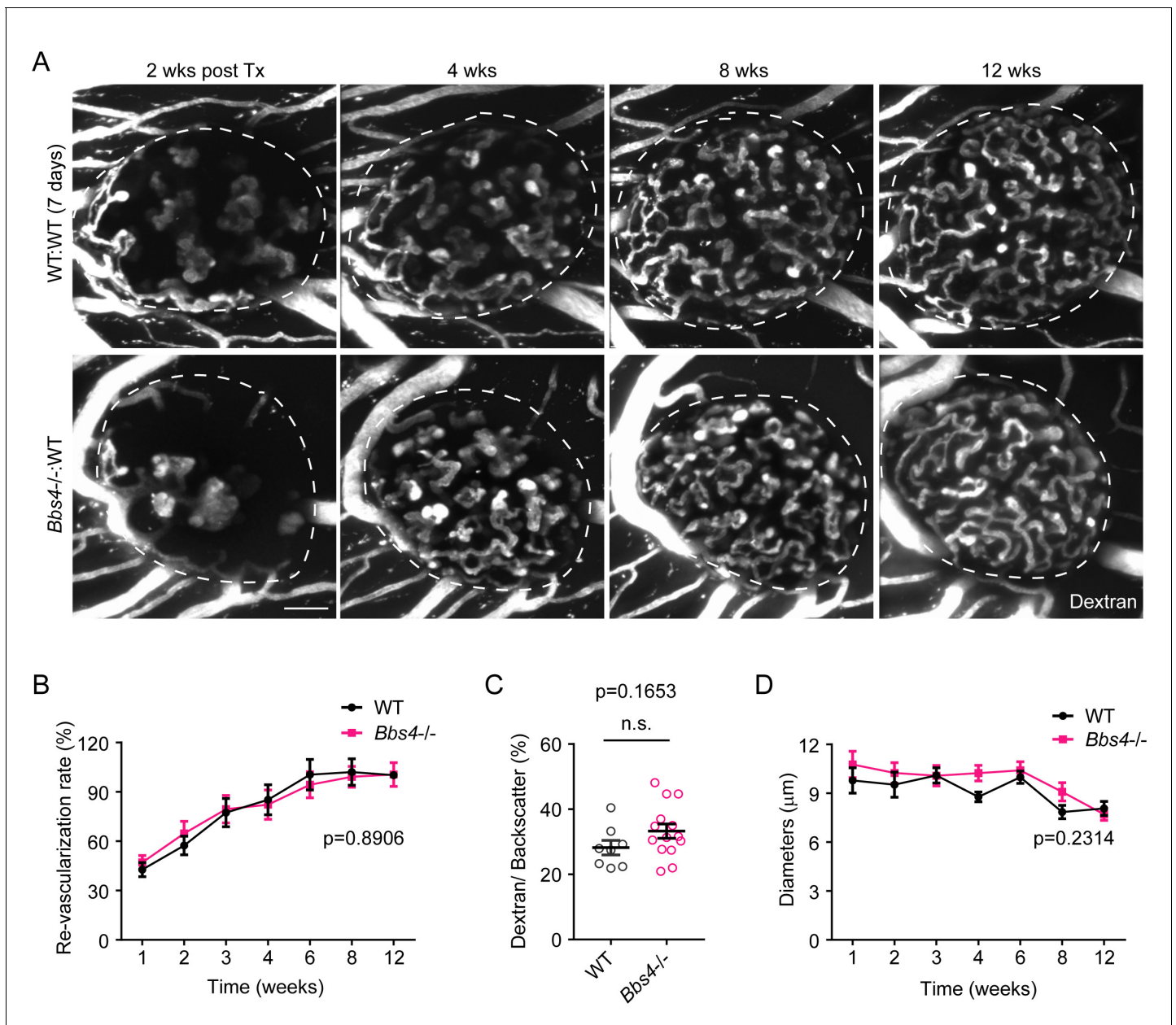


Figure 2. *Bbs4*^{-/-} islets after prolonged culture exhibit normal re-vascularization patterns in wt recipient eyes. (A) Re-vascularization of 7-day-cultivated wt (upper) and *Bbs4*^{-/-} (lower) islets in wt recipient eyes at 2-, 4-, 8- and 12-weeks post-transplantation, visualized by intravenous injection of Texas Red-conjugated dextran. Donor islets have been cultured for 7 days prior to transplantation. (B) Quantification of re-vascularization rates of wt and *Bbs4*^{-/-} islet grafts in wt recipients. Results are mean ± S.E.M. (C) Relative vascular density of wt and *Bbs4*^{-/-} islet grafts at the end of 12 weeks post-transplantation. Individual data points are shown, n.s. means not significant by Mann-Whitney test. (D) Average diameters of newly formed capillaries in wt and *Bbs4*^{-/-} islet grafts in wt recipients. Results are mean ± S.E.M., n = 4 for animals and n = 2–6 islets per animal. Scale bar: 50 μm.

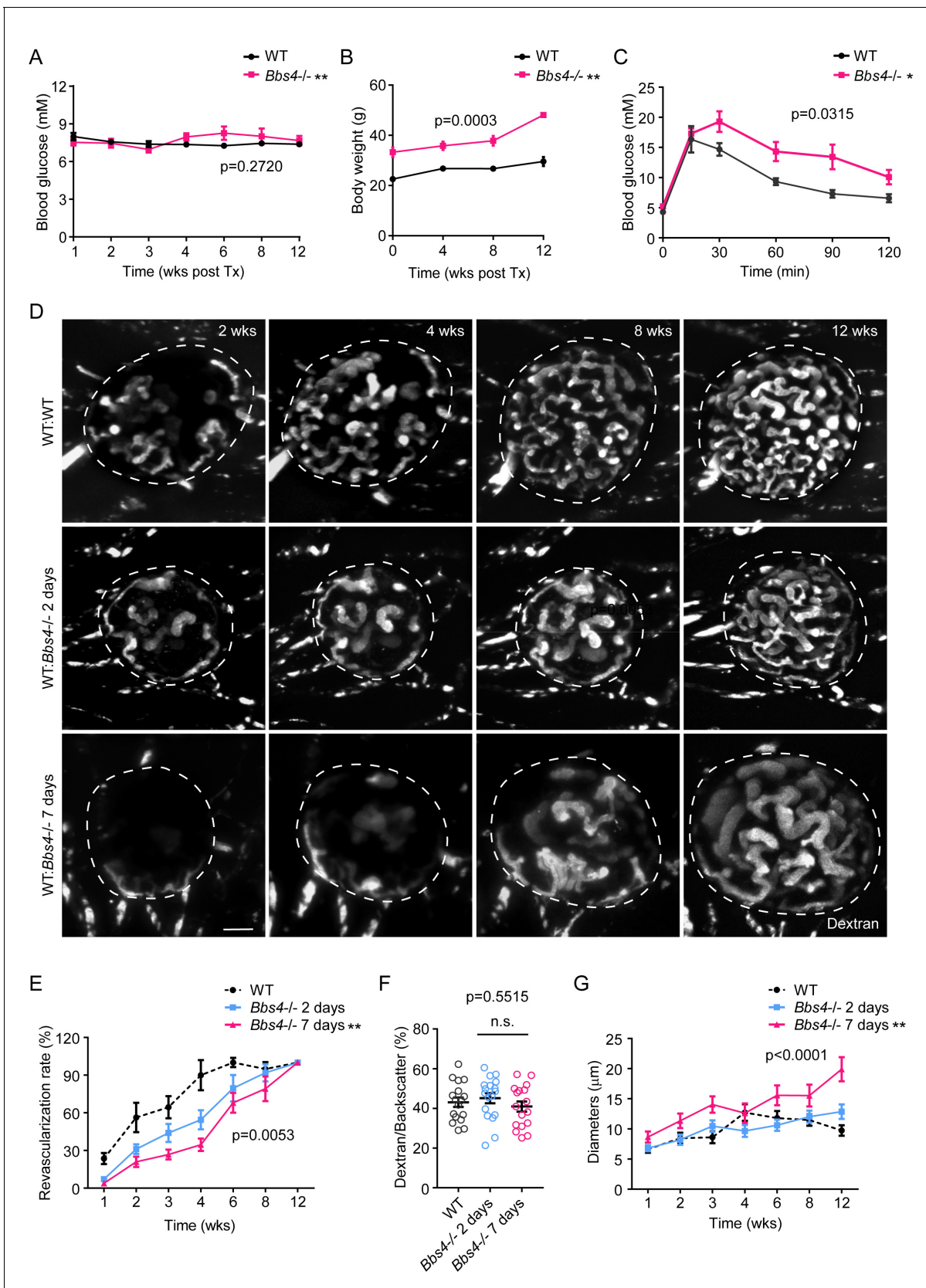


Figure 3. Wildtype islet grafts transplanted into *Bbs4*^{-/-} recipient eyes show stronger impairment in re-vascularization. (A) Non-fasting glycemic levels in *Bbs4*^{-/-} mice during islet engraftment. (B) Body weight measurements of *Bbs4*^{-/-} mice during engraftment. (C) Intraperitoneal glucose tolerance test 12 weeks post-transplantation. (D) Fluorescence microscopy images of islet grafts at 2, 4, 8, and 12 weeks post-transplantation. (E) Revascularization rates at 12 weeks post-transplantation. (F) Dextran/Backscatter at 12 weeks post-transplantation. (G) Vessel diameters at 12 weeks post-transplantation. Figure 3 continued on next page

Figure 3 continued

weeks post-transplantation. Results are mean \pm S.E.M. * $p < 0.05$, ** $p < 0.01$ by two-way-ANOVA, $n = 5$. (D) Re-vascularization of wt islets (upper) after 2 (middle) or 7 days (lower) of culture in wt or *Bbs4*^{-/-} recipients at 2-, 4-, 8- and 12-weeks post-transplantation, visualized by intravenous injection of Texas Red-conjugated dextran. (E) Quantification of re-vascularization rates of wt islet grafts. Results are mean \pm S.E.M. (F) Relative vascular density of wt islet grafts in different recipients at the end of 12 weeks post-transplantation. Individual data points are shown, n.s. means not significant by one-way-ANOVA. (G) Average diameters of newly formed capillaries in wt islet grafts. Results are mean \pm S.E.M. Comparisons were made between 2 day and 7 day groups by two-way-ANOVA, * $p < 0.05$, ** $p < 0.01$. $n = 4$ for animals and $n = 2-4$ islets per animal for wt recipients. $n = 5$ for animals and $n = 1-4$ islets per animal for *Bbs4*^{-/-} recipients. Scale bar: 50 μm .

Figure 3—figure supplement 1 continued

overlaps. (B) Representative images showing that 2-day and 7-day cultivation of *Cdh-tdT* islets leads to different amounts of donor endothelial cells constituting islet vasculature after engraftment. (C) Re-vascularization of 2-day-cultivated wt (upper) and *Bbs4*^{-/-} (lower) islets in *Cdh-tdT* recipient eyes at 2-, 4-, 8- and 12-weeks post-transplantation, visualized by intravenous injection of FITC-conjugated dextran. (D) Quantification of re-vascularization rates of wt and *Bbs4*^{-/-} islet grafts in *Cdh-tdT* recipients. (E) Average diameters of newly formed capillaries in wt and *Bbs4*^{-/-} islet grafts in wt recipients. (F) Proportion of recipient to donor endothelial cells in wt and *Bbs4*^{-/-} islet grafts indicated by the surface area ratio of tdTomato labeled cells to total dextran labeled islet vessels during engraftment. Results are mean ± S.E.M. * $p < 0.05$, ** $p < 0.01$ by two-way ANOVA, $n = 5$ for animals and $n = 2-4$ islets per animal. Scale bars: 50 μm .

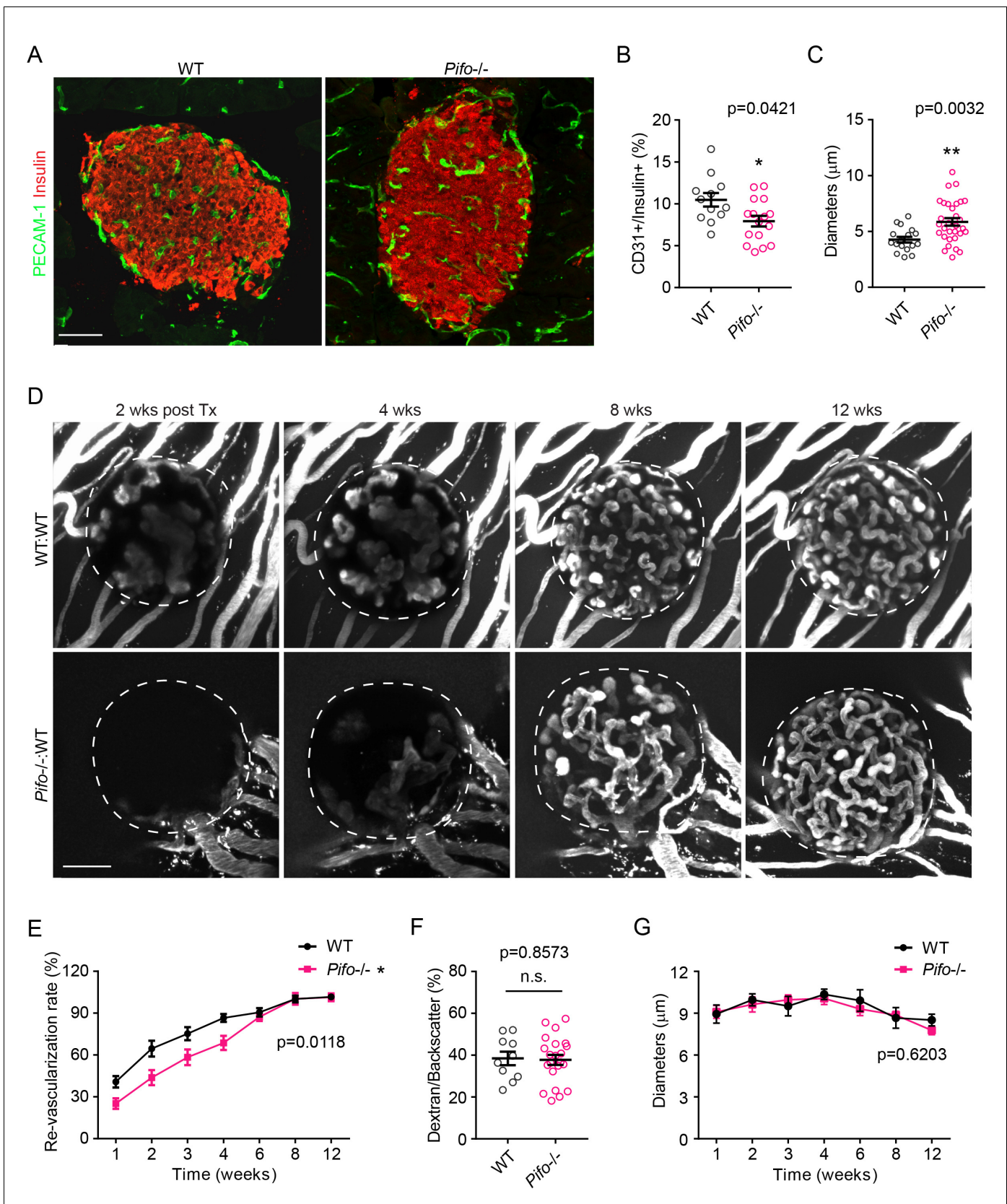


Figure 3—figure supplement 2. *Pif0*^{-/-} mice exhibit similar islet vascular phenotypes as *Bbs4*^{-/-} mice. (A) Immuno-fluorescence staining of pancreatic sections from 3-month-old wt and *Pif0*^{-/-} mice showing islets (insulin, red) and intra-islet capillaries (PECAM-1, green). (B–C) Quantification of relative Figure 3—figure supplement 2 continued on next page

Figure 3—figure supplement 2 continued

intra-islet PECAM-1 positive volume, normalized to insulin-positive volume (B) and average intra-islet capillary diameters (C) in wt and *Pifo*^{-/-}-pancreatic sections. Individual data points are shown. * $p < 0.05$, ** $p < 0.01$ by Mann-Whitney test, $n = 3$ for animals and $n = 4$ –6 islets per animal. (D) Re-vascularization of 2-day-cultivated wt (upper) and *Pifo*^{-/-} (lower) islets in wt recipient eyes at 2-, 4-, 8- and 12-weeks post-transplantation, visualized by intravenous injection of Texas Red-conjugated dextran. (E) Quantification of re-vascularization rates of wt and *Pifo*^{-/-}-islet grafts in wt recipients. Results are mean \pm S.E.M. (F) Relative vascular density of wt and *Pifo*^{-/-}-islet grafts at the end of 12 weeks post-transplantation. Individual data points are shown. (G) Average diameters of newly formed capillaries in wt and *Pifo*^{-/-}-islet grafts in wt recipients. Results are mean \pm S.E.M., ** $p < 0.01$ by two-way ANOVA, n.s. means not significant by Mann-Whitney test, $n = 5$ for animals and $n = 2$ –5 islets per animal. Scale bars: 50 μ m.

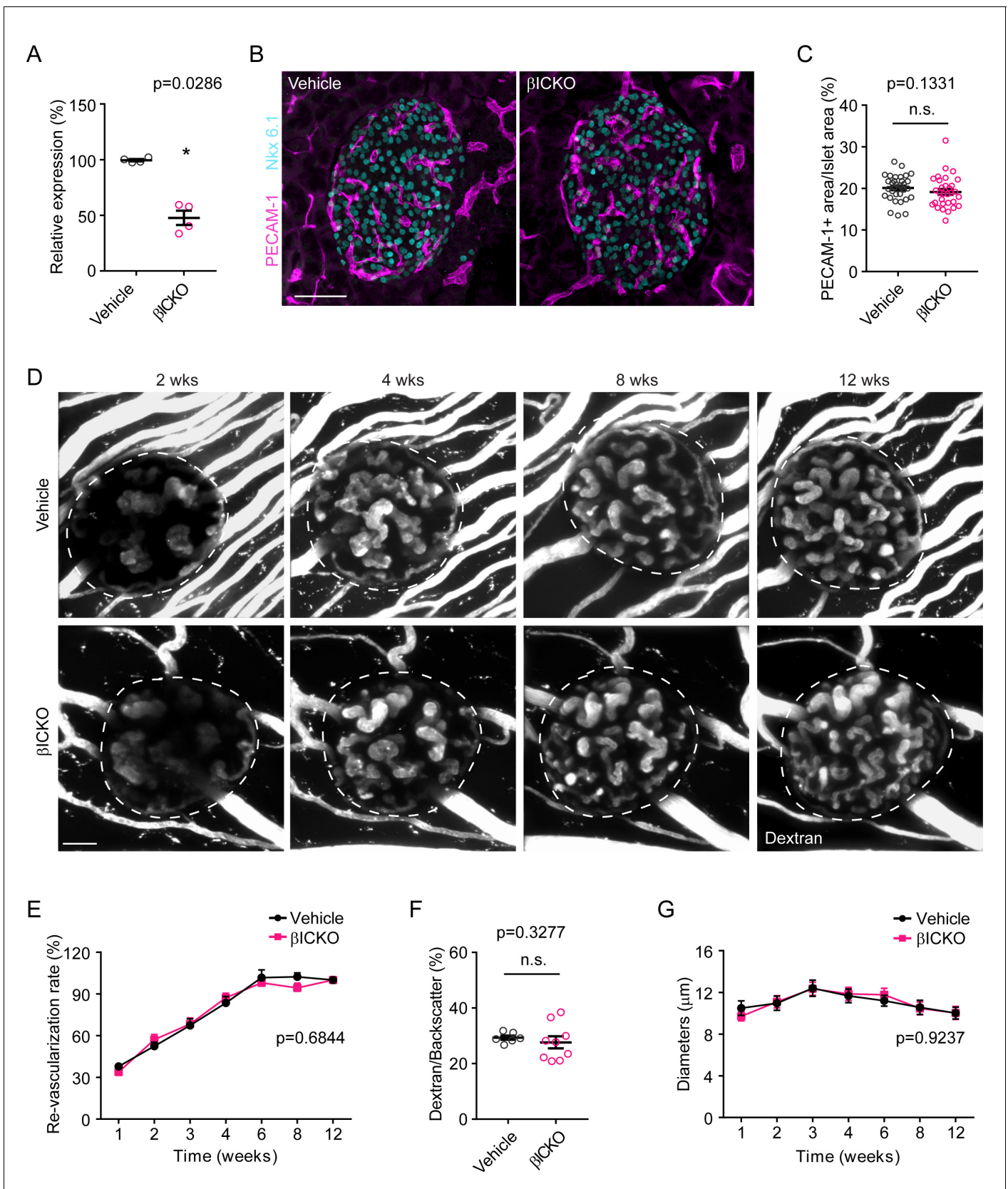


Figure 4. β ICKO mice display no visible islet vascular phenotypes. (A) Efficiency of *Ift88* silencing by tamoxifen induction. Individual data points are shown, ** $p < 0.01$ by Mann-Whitney test, $n = 4$ for animals. (B) Immuno-fluorescence staining of pancreatic sections from 2-month-old control (vehicle) Figure 4 continued on next page

Figure 4 continued

and β ICKO mice, showing islets (Nkx 6.1, cyan) and intra-islet capillaries (PECAM-1, magenta). (C) Quantification of relative intra-islet PECAM-1 positive area, normalized to islet area in control and β ICKO pancreatic sections. Individual data points are shown, n.s. means not significant by Mann-Whitney test, $n = 6$ for animals and $n = 5-6$ islets per animal. (D) Re-vascularization of overnight-cultured control (upper) and β ICKO (lower) islets in wt recipient eyes at 2-, 4-, 8- and 12-weeks post-transplantation, visualized by intravenous injection of Texas Red-conjugated dextran. (E) Quantification of re-vascularization rates of control and β ICKO islet grafts in wt recipients. Results are mean \pm S.E.M. $n = 6$ for animals and $n = 6-8$ islets per animal. (F) Relative vascular density of control and β ICKO islet grafts at the end of 12 weeks post-transplantation. Individual data points are shown. $n = 3$ for animals and $n = 2-3$ islets per animal. (G) Average diameters of newly formed capillaries in control and β ICKO islet grafts in wt recipients. Results are mean \pm S.E.M. and n.s. means not significant by Mann-Whitney test. $n = 6$ for animals and $n = 6-8$ islets per animal. Scale bars: 50 μ m.

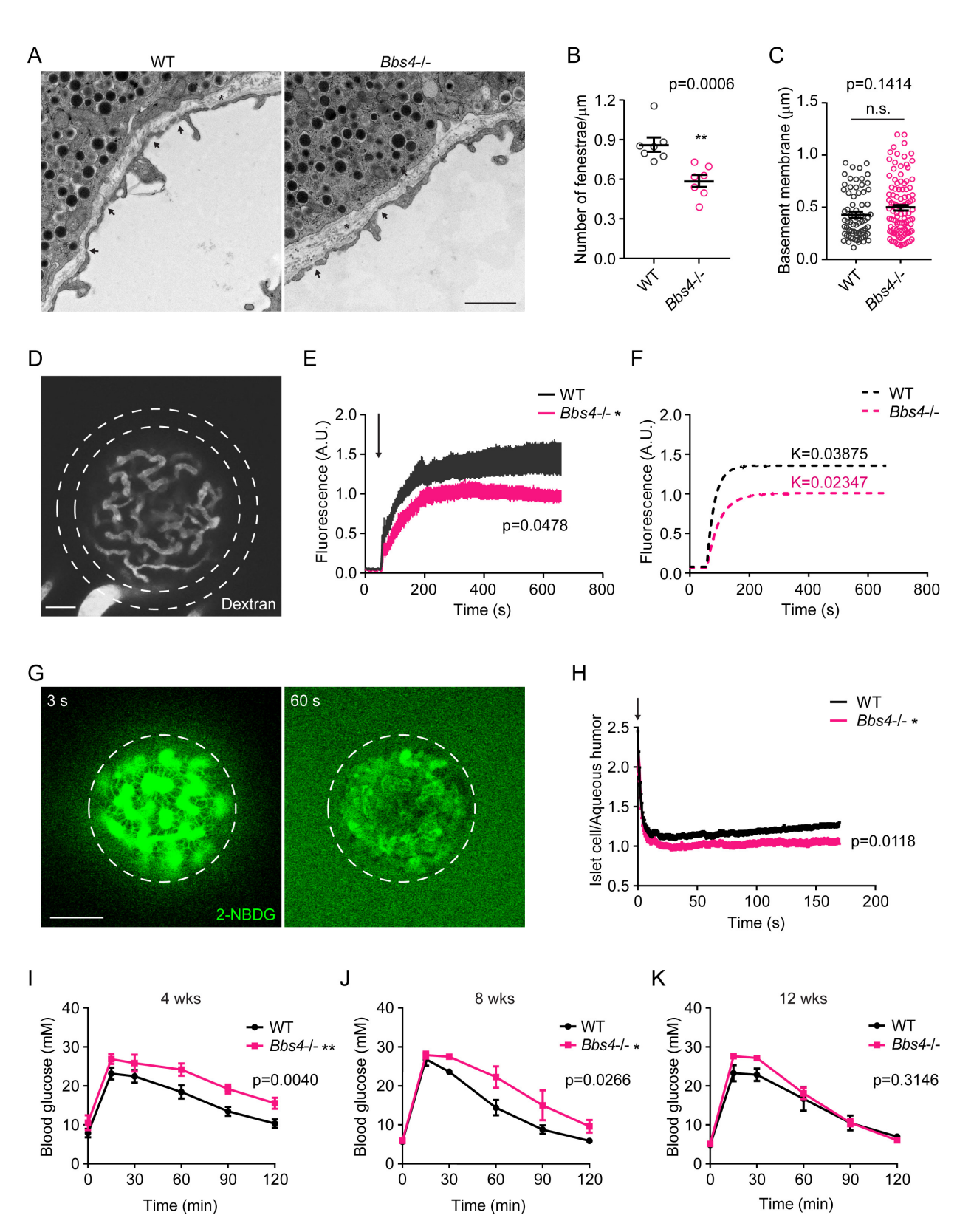


Figure 5. Dysfunctional intra-islet vasculature in *Bbs4*^{-/-} islets undermines glucose metabolism. (A) Electron microscopic images of wt and *Bbs4*^{-/-} islet graft dissected from wt recipient eyes, showing fenestrated islet capillaries (arrows) and basement membrane (asterisks). Scale bar: 1 μ m. (B–C) Figure 5 continued on next page

Figure 5 continued

Quantification of average fenestrae density (B) and basement membrane thickness (C) of the capillaries in wt and *Bbs4*^{-/-} islet grafts. Individual data points are shown, **p<0.01, n.s. means not significant by Mann-Whitney test, n = 7 for animals, and n = 1–2 for islets. (D) Representative image showing leakage of 40 KDa FITC-conjugated dextran from wt islet grafts in mouse eyes at 1 min after injection. Scale bar: 50 μm. (E–F) Quantification of FITC fluorescence intensity in the region circles by the dashed lines outside wt and *Bbs4*^{-/-} islet grafts (E) and simulated curves showing different kinetics (F). Arrow indicates injection time point. Results are mean ± S.E.M. *p<0.05 by two-way-ANOVA, n = 12 for animals. (G) Representative image showing 2-NBDG leakage from wt islet vasculature and uptake by islet cells in vivo. Times points are 3 s (left) and 60 s (right) after injection. Scale bar: 50 μm. (H) Real-time ratio of 2-NBDG fluorescence intensity in islet cells of wt and *Bbs4*^{-/-} islet grafts to aqueous humor. Arrow indicates injection time point. Results are mean ± S.E.M. *p<0.05, n = 8 for animals and n = 1–2 for islets. (I–K) Intraperitoneal glucose tolerance test of wt recipient mice which were transplanted with wt or *Bbs4*^{-/-} islets, at 4 weeks (I), 8 weeks (J) and 12 weeks (K) post-transplantation. Results are mean ± S.E.M. *p<0.05, **p<0.01 by two-way-ANOVA, n = 6 for animals.

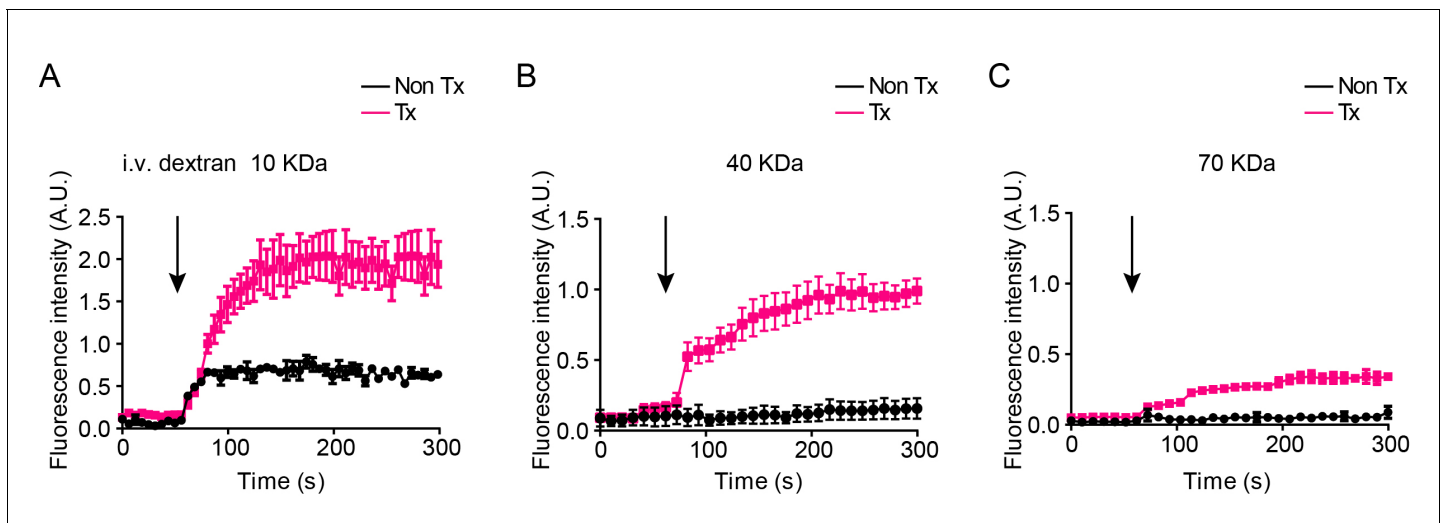


Figure 5—figure supplement 1. Dextran leakage kinetics from the capillaries of islet grafts or the iris vessels in mouse eyes. Kinetics of fluorescence intensity outside islet grafts in transplanted eyes (Tx) or in the aqueous humor of non-transplanted control eyes (Non-Tx) after intravenously injection of fluorescently labeled dextran at sizes of 10 KDa (A), 40 KDa (B) and 70 KDa (C), respectively. Results are mean \pm S.E.M, n = 4.

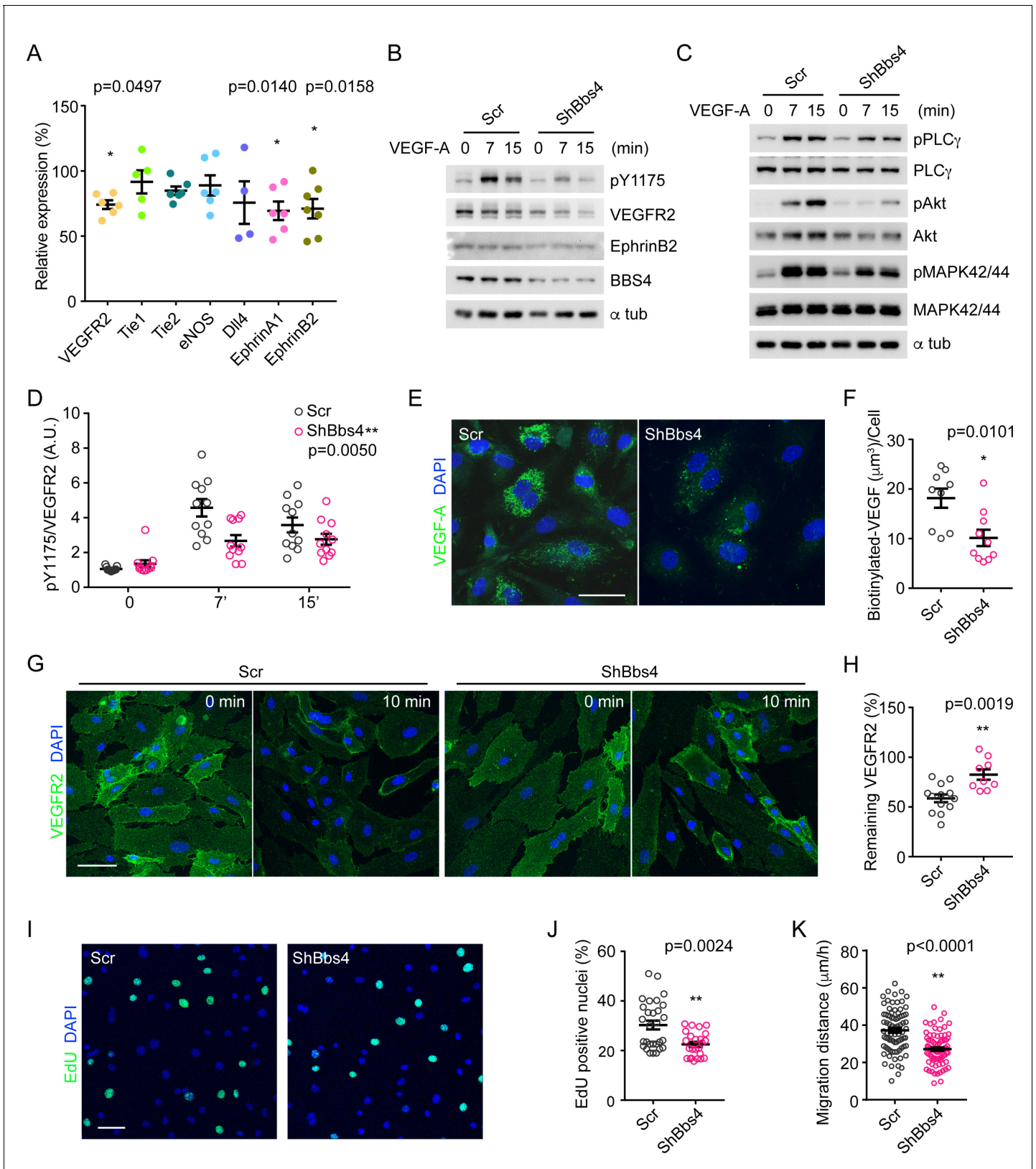


Figure 6. VEGFA-VEGFR2 induced signaling pathway and angiogenic response is disrupted in *Bbs4* silenced endothelial cells. (A) qPCR analysis of VEGF-A signaling related gene expression in *Bbs4* silenced MS-1. Results are presented as relative mRNA levels normalized to scrambled shRNA treated cells, * $p<0.05$, ** $p<0.01$ by one-way-ANOVA, $n = 3$. (B) and (C) Western blots showing VEGF-A signaling pathway in scrambled or shBbs4 treated cells. (D) pY1175/VEGFR2 ratio. (E) VEGF-A staining. (F) Biotinylated-VEGF uptake. (G) VEGFR2 staining at 0 and 10 min. (H) Remaining VEGFR2. (I) EdU staining. (J) EdU positive nuclei. (K) Migration distance. Figure 6 continued on next page

Figure 6 continued

treated HDMECs. (D) Quantification of VEGFR2 activation. (E) Representative images showing biotinylated VEGF-A uptake in scrambled or ShBbs4 treated HDMECs and quantification (F). (G) Representative cell surface staining of VEGFR2 in scrambled (Scr) or ShBbs4 treated HDMECs, prior to (0 min) and after VEGF-A stimulation (10 min). (H) Quantification of the percentage of remaining membrane-bound VEGFR2. (I) VEGF-A induced proliferation in Scr or ShBbs4 treated MS-1 by EdU assay (green) and quantification (J). (K) VEGF-A induced endothelial cell migration in Scr or ShBbs4 treated MS-1. Individual data points are shown, * $p < 0.05$, ** $p < 0.01$ by Mann-Whitney test, $n = 3$. Scale bars: 50 μm .

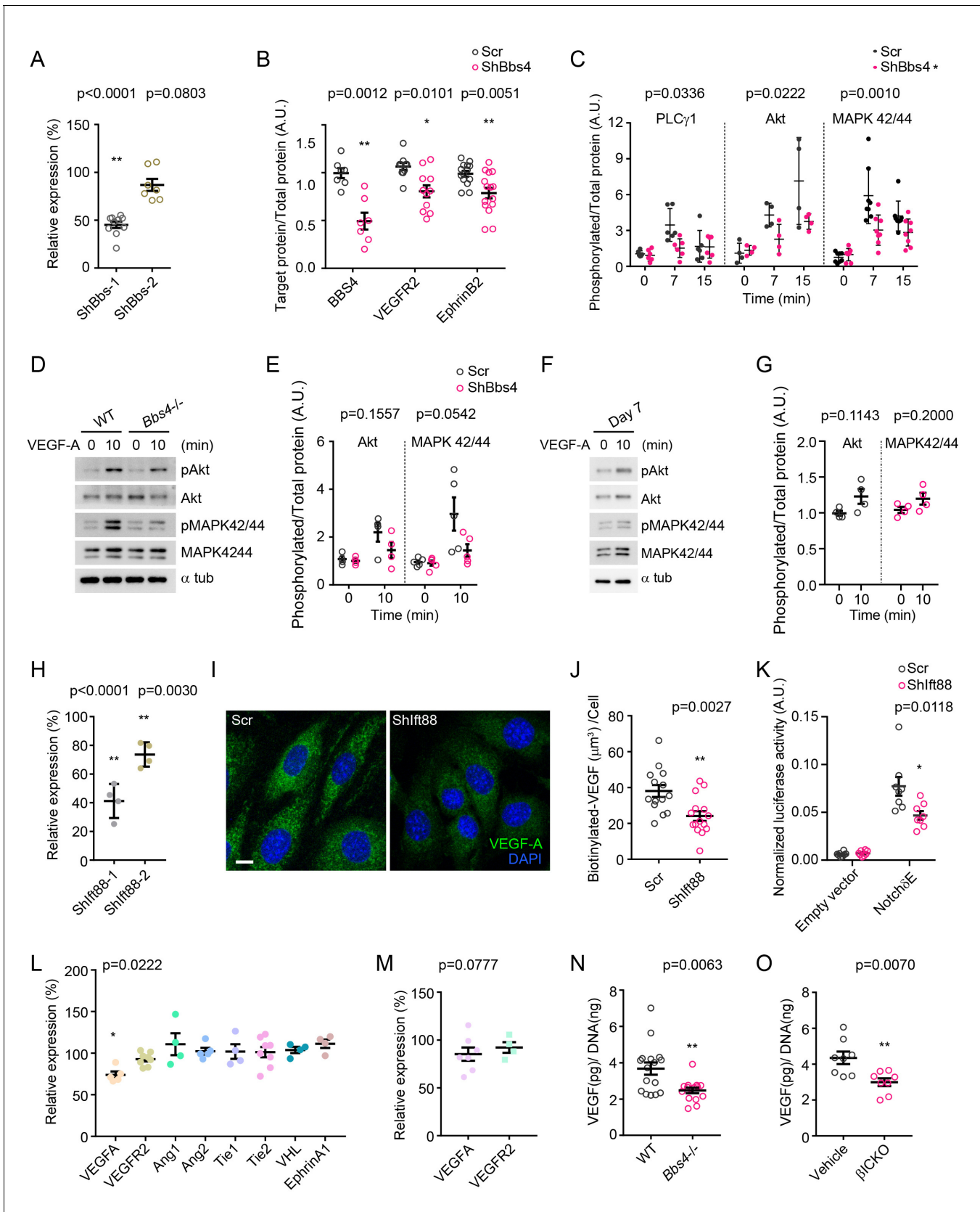


Figure 6—figure supplement 1. VEGF-A gene expression, secretion and signaling in *Bbs4* or *Ift88* depleted cells. (A) Efficiency of shRNA silencing of *Bbs4* in MS-1 endothelial cells. Individual data points are shown, ** $p < 0.01$ by one-way-ANOVA, $n = 4$. (B–C) Quantification of western blots showing Figure 6—figure supplement 1 continued on next page

Figure 6—figure supplement 1 continued

BBS4, VEGFR2 and EphrinB2 protein levels (B), and activation of PLC γ 1, Akt and MAPK 42/44 (C) in scrambled or shBbs4 treated HDMECs. * $p < 0.05$, ** $p < 0.01$ by two-way-ANOVA, $n = 3$. (D) Western blots showing VEGF-A signaling pathway in freshly isolated wt and *Bbs4*^{-/-} islets, and (E) quantification of activation of Akt and MAPK 42/44. * $p < 0.05$ by two-way-ANOVA, $n = 3$ for animals. (F) Western blots showing VEGF-A signaling pathway in isolated wt islets cultivated for 7 days, and (G) quantification of activation of Akt and MAPK 42/44, * $p < 0.05$ by Mann-Whitney test, $n = 2$ for animals. (H) Efficiency of shRNA silencing of *Ift88* in MS-1 cells. ** $p < 0.01$ by one-way-ANOVA, $n = 3$. (I) Representative images showing biotinylated VEGF-A uptake in scrambled or Shft88 treated MS-1 cells and quantification (J), ** $p < 0.01$ by Mann-Whitney test, $n = 3$. Scale bar: 10 μ m. (K) Notch signaling activity in scrambled or Shft88 treated MS-1 cells and indicated by luciferase assay. * $p < 0.05$ by Mann-Whitney test, $n = 3$. (L) qPCR analysis of angiogenic gene expression in freshly isolated wt and *Bbs4*^{-/-} islets. ** $p < 0.01$ by one-way-ANOVA, $n = 4$ for animals. (M) qPCR analysis of VEGF-A and VEGFR2 gene expression in freshly isolated control and β ICKO islets. Results are presented as relative mRNA levels normalized to control. * $p < 0.05$ by one-way-ANOVA, $n = 4$ for animals. (N) VEGF-A secretion from cultured wt and *Bbs4*^{-/-} islets, normalized to total DNA quantity of islets. ** $p < 0.01$ by Mann-Whitney test, $n = 5$ for animals. (O) VEGF-A secretion from cultured control and β ICKO islets, normalized to total DNA quantity of islets. ** $p < 0.01$ by Mann-Whitney test, $n = 4$ for animals.